

<https://helda.helsinki.fi>

A Predictive Model for Steady State Ozone Concentration at an Urban-Coastal Site

Alghamdi, Mansour A.

Multidisciplinary Digital Publishing Institute
2019-01-17

Alghamdi, M.A.; Al-Hunaiti, A.; Arar, S.; Khoder, M.; Abdelmaksoud, A.S.; Al-Jeelani, H.; Lihavainen, H.; Hyvärinen, A.; Shabbaj, I.I.; Almeahmadi, F.M.; Zaidan, M.A.; Hussein, T.; Dada, L. A Predictive Model for Steady State Ozone Concentration at an Urban-Coastal Site. *Int. J. Environ. Res. Public Health* 2019, 16, 258.

<http://hdl.handle.net/10138/348470>

Downloaded from Helda, University of Helsinki institutional repository.

This is an electronic reprint of the original article.



This reprint may differ from the original in pagination and typographic detail.

Please cite the original version.



Article

A Predictive Model for Steady State Ozone Concentration at an Urban-Coastal Site

Mansour A. Alghamdi ¹, Afnan Al-Hunaiti ², Sharif Arar ², Mamdouh Khoder ¹, Ahmad S. Abdelmaksoud ¹, Hisham Al-Jeelani ¹, Heikki Lihavainen ³, Antti Hyvärinen ³, Ibrahim I. Shabbaj ¹, Fahd M. Almeahmadi ¹, Martha A. Zaidan ⁴, Tareq Hussein ^{4,5} 
and Lubna Dada ^{4,*} 

¹ Department of Environmental Sciences, Faculty of Meteorology, Environment and Arid Land Agriculture, King Abdulaziz University, P.O. Box 80208, Jeddah 21589, Saudi Arabia; mghamdi2@kau.edu.sa (M.A.A.); khoder_55@yahoo.com (M.K.); asabdelmaksoud@yahoo.com (A.S.A.); hjeelani@gmail.com (H.A.-J.); ishabbaj@yahoo.com (I.I.S.); fmeahmadi@gmail.com (F.M.A.)

² Department of Chemistry, University of Jordan, Amman 11942, Jordan; a.alhunaiti@ju.edu.jo (A.A.-H.); s.arar@ju.edu.jo (S.A.)

³ Finnish Meteorological Institute, Erik Palménin aukio 1, FI-00101 Helsinki, Finland; heikki.lihavainen@fmi.fi (H.L.); antti.hyvarinen@fmi.fi (A.H.)

⁴ Institute for Atmospheric and Earth System Research (INAR), University of Helsinki, FI-00014 Helsinki, Finland; martha.zaidan@helsinki.fi (M.A.Z.); tareq.hussein@helsinki.fi (T.H.)

⁵ Department of Physics, University of Jordan, Amman 11942, Jordan

* Correspondence: Lubna.dada@helsinki.fi; Tel.: +358504488568

Received: 27 September 2018; Accepted: 15 January 2019; Published: 17 January 2019



Abstract: Ground level ozone (O_3) plays an important role in controlling the oxidation budget in the boundary layer and thus affects the environment and causes severe health disorders. Ozone gas, being one of the well-known greenhouse gases, although present in small quantities, contributes to global warming. In this study, we present a predictive model for the steady-state ozone concentrations during daytime (13:00–17:00) and nighttime (01:00–05:00) at an urban coastal site. The model is based on a modified approach of the null cycle of O_3 and NO_x and was evaluated against a one-year data-base of O_3 and nitrogen oxides (NO and NO_2) measured at an urban coastal site in Jeddah, on the west coast of Saudi Arabia. The model for daytime concentrations was found to be linearly dependent on the concentration ratio of NO_2 to NO whereas that for the nighttime period was suggested to be inversely proportional to NO_2 concentrations. Knowing that reactions involved in tropospheric O_3 formation are very complex, this proposed model provides reasonable predictions for the daytime and nighttime concentrations. Since the current description of the model is solely based on the null cycle of O_3 and NO_x , other precursors could be considered in future development of this model. This study will serve as basis for future studies that might introduce informing strategies to control ground level O_3 concentrations, as well as its precursors' emissions.

Keywords: chemical coupling; nitrogen oxides; ozone; weekend effect

1. Introduction

Tropospheric ozone (O_3) is known for causing severe health effects and having environmental impacts [1,2]. Among other photochemical oxidants, O_3 is one of the widely studied subjects worldwide under the category of air pollution. Besides that, O_3 is a key precursor of hydroxyl radicals (OH), which control the oxidizing power of the lower atmosphere and by that alters its chemical properties [3].

Ground level O_3 formation depends on photochemistry, meteorological conditions, and air mass transport [4–7]. For instance, O_3 is found to peak during the summer time accompanying high

temperatures and long daytime hours and thus seems to be correlated with solar radiation intensity [8–13]. In urban environments, the diurnal cycle of O_3 consists of nighttime low concentrations and daytime high concentrations, which may last for several hours (Figure 1). This high O_3 concentration during the daytime is mainly attributed to photochemical reactions mainly within the NO_x – O_3 cycle. The low O_3 concentrations during nighttime are the result of the pause in ozone production, due to the absence of photochemical reactions. Eventually, the O_3 is recycled through chemical reactions or is lost by deposition [14]. It is interesting that the daytime steady-state O_3 concentration on weekends is higher than that on workdays. The latter can be attributed to higher traffic on workdays than on weekends, releasing more NO_x , which in turn uses up the daytime available ozone, leaving behind a lower concentration of steady state ozone on workdays. The aforementioned assumptions are discussed in more detail in the following sections. Being the major source of daytime ground level O_3 , we believe that the NO_x – O_3 null cycle, can be applied to predict the steady-state daytime O_3 concentrations in urban areas.

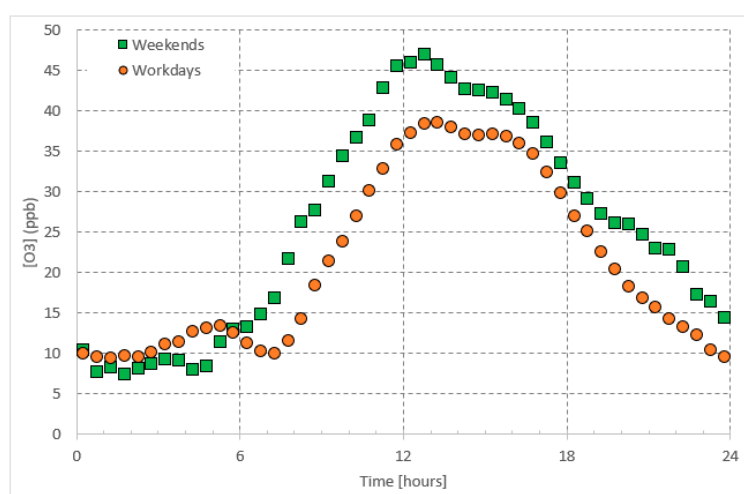


Figure 1. Average daily pattern of O_3 presented separately for workdays and weekends.

The momentary change rate of O_3 concentrations can be described by its sources and sinks involved in atmosphere [15,16]. For instance, in urban environments, O_3 is formed through a series of daytime reactions that involve NO_x (NO and NO_2), which are of anthropogenic origin. Other sources of O_3 include volatile organic compounds ($VOCs$) and carbon monoxide (CO) [17]. The priority of the reactions depends on the concentrations of NO_x and $VOCs$, as well as the ratio of the two (NO_x/VOC) [18]. Accordingly, two regimes for O_3 formation have been proposed. The first one is the NO_x -sensitive regime in which the increase in NO_x concentration causes an increase in O_3 concentration and the formation of O_3 is mainly independent of the $VOCs$ concentration. The second one is the VOC -sensitive regime in which the O_3 formation is solely dependent on the $VOCs$ concentration [19,20]. Therefore, the prevailing regime is specific to the dominant environmental conditions.

In the urban atmosphere, NO and NO_2 are emitted from anthropogenic activities, including combustion processes (e.g., traffic and industrial activities). Their daily patterns (Figures 2 and 3) are, therefore, controlled by these emissions [21–23]. Since NO is a primary pollutant and acts to form NO_2 upon a series of reactions [24], the NO_2 morning peak appears one hour later than the NO peak. The NO_x concentrations vary between morning and evening and the change is attributed to many factors. First, during the early hours of daytime, high traffic emissions are accumulated in the atmosphere when the photo-chemically produced O_3 concentrations are still low; O_3 acts as a sink for both NO and NO_2 . Concurrent with sunrise, these pollutants are consumed with daytime produced O_3 and are subject to thermal turbulence, due to higher temperature resulting in their dilution, dispersion within expansion in the boundary layer and eventually a drop in their concentrations [25,26]. On the

other hand, along with sunset NO and NO_2 encounter lower temperature, less boundary layer mixing and low dispersion leading to an increase in their concentrations.

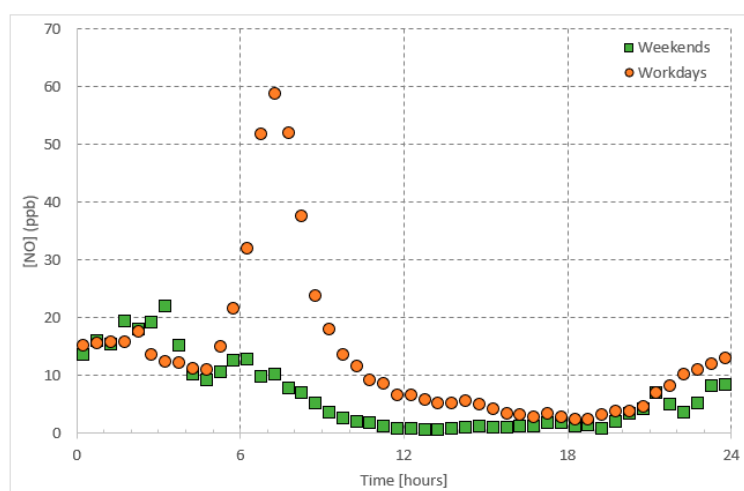


Figure 2. Average daily pattern of NO presented separately for workdays and weekends.

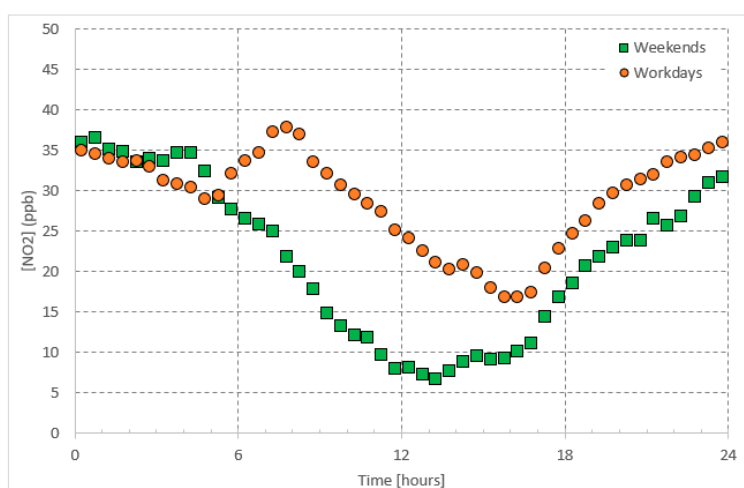


Figure 3. Average daily pattern of NO_2 presented separately for workdays and weekends.

The characteristics and patterns of ground level O_3 have been the subject of many studies worldwide [27]. Specifically, the chemical coupling between O_3 and its precursors (NO and NO_2) was investigated thoroughly in urban environments [19,22,28–31]. However, very few studies considered modelling of ground level O_3 [32–35]. In fact, O_3 is involved in many chemical reactions that sometimes make its prediction very difficult. In this study, we present a simple statistical predictive model to calculate the steady-state daytime and nighttime O_3 concentrations at an urban coastal site. For the purpose of model evaluation, we utilized a one-year data-base of ozone (O_3) and nitrogen oxides (NO and NO_2) measured in Jeddah, which is located on the western part of Saudi Arabia [36]. Our model could be modified to evaluate ozone in other urban environments with similar diurnal patterns.

2. Materials and Methods

2.1. Simple Statistical Predictive Model

In the troposphere, ozone (O_3) and nitrogen oxides (NO_x) undergo a well-known null cycle in which each gaseous species maintains a steady-state concentration [37]; i.e., balanced production and loss rates balance each other (Figures 1–3). As postulated in the introduction, the daytime steady-state

O_3 concentration is higher than that during the nighttime steady-state concentrations. Furthermore, the chemical reactions involved with the O_3 are different during both periods. Therefore, we postulate the simple predictive model for two time periods: Daytime and nighttime.

2.2. Daytime Steady-State O_3 Concentrations Prediction

Under atmospheric conditions and in the presence of solar radiation ($\lambda < 424$ nm), the O_3 - NO_x null cycle includes three successive reactions [37]:



where M is an inert ground state (either N_2 or O_2) that acts as a surface for the reaction to take place and M^* is the excited state of the molecule, hv is the energy of the solar radiation photons that induces photochemical oxidation, O is known to be highly reactive and disappears as soon as it is generated. Here, the concentration of O_2 is assumed to be constant.

Under steady-state conditions, the null cycle has the steady-state formula,

$$\frac{J_{NO_2}}{k_3} = \frac{[NO][O_3]}{[NO_2]}, \quad (2)$$

where J_{NO_2} is the rate coefficient of NO_2 photolysis, k_3 is the reaction rate coefficient of O_3 and NO . It is well known that the k_3 is temperature dependent [38]; $k_3 = 3.23 \exp(-1430/T)$ in units of $ppb^{-1}min^{-1}$. However, the seasonal temperature variation is few degrees; and therefore, we do not expect k_3 to have a considerable variation throughout the year in Jeddah.

Re-arrangement of Equation (2) yields a simple equation to predict the concentration of O_3 from the ratio of NO_2 to NO concentrations during daytime,

$$[O_3] = \alpha \frac{[NO_2]}{[NO]} + \delta_1, \quad (3)$$

where α is a constant equivalent to J_{NO_2}/k_3 and δ_1 (ppb) is also constant related to the background O_3 concentrations (e.g., migrates from the stratosphere to the troposphere, long-range transport, product of other reactions).

During daytime steady-state, using Equation (1):

$$\frac{d[NO_2]}{dt} = -J_{NO_2}[NO_2] + k_3[O_3][NO] = 0, \quad (4)$$

Upon rearranging we get Equation (2). We then compute a linear regression of $[O_3]$ vs. $[NO_2/NO]$ of measured data. We, thus, are able to derive the constants for the model as $y = ax + b$ (Equation (3)), where a is a constant equivalent to J_{NO_2}/k_3 and b is also constant related to the background O_3 concentrations.

2.3. Nighttime Steady-State O_3 Concentrations Prediction

During night-time hours, O_3 is mainly consumed through its reaction with NO_2 ,



Applying reaction rate kinetics and rearrangement of the Equation (4) yields a simple equation to predict the nighttime O_3 based on the concentration of its major nighttime sink compound NO_2 ,

$$[O_3] = \beta \frac{1}{[NO_2]} - \delta_2, \quad (6)$$

where $\beta(\text{ppb}^2)$ is a constant equivalent to the reaction rate of O_3 with NO_2 and $\delta_2(\text{ppb})$ is again a constant related to the background O_3 concentrations during the night.

During nighttime, Equation (4) steady state conditions are:

$$\frac{d[O_3]}{dt} = k_{(NO_2, O_3)}[O_3][NO_2] = 0, \quad (7)$$

Upon rearranging we get Equations (6) and (7). We then compute a linear regression of $[O_3]$ vs. $[NO_2]$ of measured data. We, thus, are able to derive the constants for the model as $y = ax + b$ (Equation (3)), where a is a constant equivalent to k (reaction rate of O_3 with NO_2) and b is again a constant related to the background O_3 concentrations.

2.4. Data-Base

In this study, we utilized a one-year data-base of O_3 and NO_x concentrations measured at an urban site in Jeddah, Saudi Arabia between 1 January and 31 December 2012 [36]. The data-base is utilized to only evaluate the above described simple predictive model for steady-state O_3 concentrations. The measurement was conducted at the King Abdul-Aziz University (KAU) campus, which is surrounded by major roads and a highway. Jeddah itself is situated on the west coast of Saudi Arabia and is considered the largest sea port on the Red Sea. Potential sources of air pollution in the city are mainly vehicle emissions (1.4 million vehicles; [39]) and industrial (oil refinery, desalination plant, power generation plant, and manufacturing industry). A lot of these emissions act as O_3 precursors; under favored meteorological conditions and abundance of solar radiation, which are available in Jeddah.

3. Results

3.1. Overview of the Daily Patterns

The O_3 concentrations showed a clear daily pattern with high concentrations during the daytime, which was as high as 39 ppb and 47 ppb on workdays (Saturday–Wednesday) and weekends (Friday), respectively (Figure 1). The nighttime (before 05:00) concentrations were between 7.5 ppb and 13.2 ppb. As mentioned before in the introduction section, higher O_3 concentrations on weekends daytime are not only attributed to the NO_x cycle, but also possibly due to differences in the concentrations of other precursors (e.g., CO and VOC). The presence of $VOCs$ changes the path of O_3 formation by altering the NO_x cycle mechanism through reactions of hydroxyl radicals, which in turn oxidize NO without the use of O_3 . The latter, along with the photolysis of NO_2 , leads to accumulation of O_3 during the daytime on weekends. Furthermore, when NO_x concentrations are high, the reaction of NO_2 and OH to give HNO_3 is favored [17], which reduces the NO_2 concentrations available for photolysis. In turn, this leads to low photolysis rate J_{NO_2} during the weekends.

Recalling Equation (2), the daily pattern of J_{NO_2}/k_3 (represented by the concentrations ratio $[O_3][NO]/[NO_2]$) is characterized by a double peak (before noon and in the afternoon). The nighttime value varied between 0.5 and 1 ppb. The daytime value was as high as 5 ppb on weekends and as high as 8 on workdays (Figure 4). As claimed before, k_3 does not have significant differences throughout the year in Jeddah; and thus, the daily pattern, shown in Figure 4, should represent the daily pattern of J_{NO_2} . In general, J_{NO_2} is the rate of photolysis of NO_2 and it seems to be lower on weekends than on workdays. In general, it has been well known that photolysis occurs more rapidly during lower PM (particulate matter) concentrations; This is mainly observed during the weekends [31,40]. The reason could be also referred to the change of both the $[NO]/[NO_2]$ ratio and the O_3 concentration

(‘weekend effect’). As shown in Figure 5, the daytime value of $[NO]/[NO_2]$ is higher on workdays than on weekends.

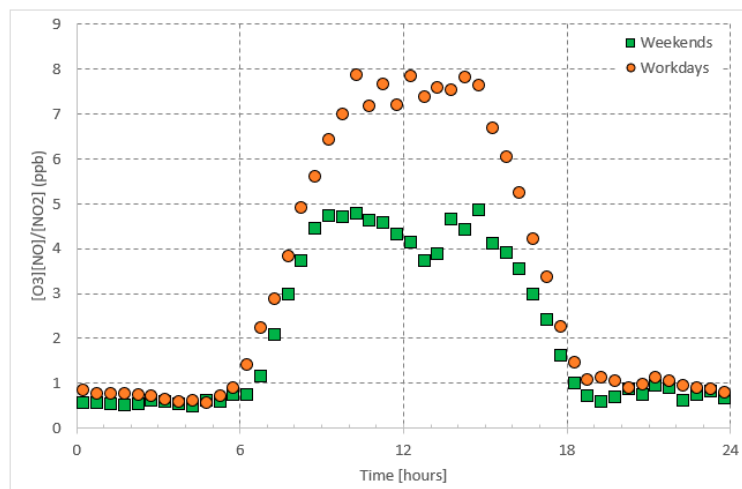


Figure 4. Average daily pattern of photo-stationary state concentrations $[NO][O_3]/[NO_2]$ presented separately for workdays and weekends.

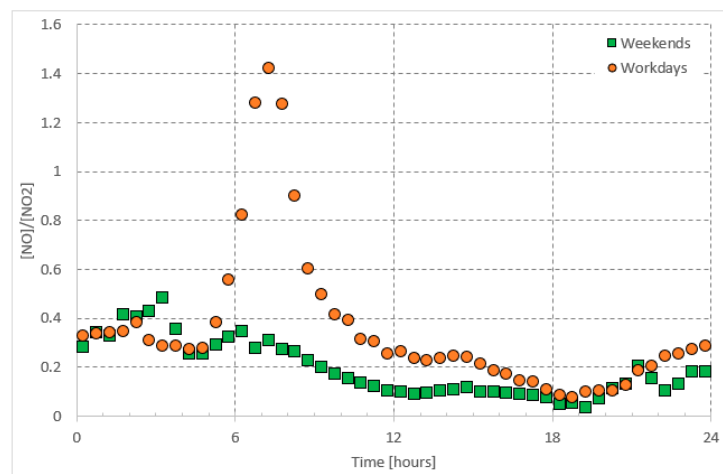


Figure 5. Average daily pattern of $[NO]/[NO_2]$ presented separately for workdays and weekends.

3.2. Prediction of Steady-State O_3 Concentration

As shown in Figures 1–3, regarding the daily pattern of O_3 and NO_x , the steady-state conditions are met during 13:00–17:00 (referred to as daytime steady-state period) and 01:00–05:00 (referred to as nighttime steady-state period). We considered the 30-minutes average of the data-base and selected these time periods separately to apply the simple predictive model, which is a linear regression model. We applied the fitting to the whole data set. The nighttime period for all weekdays was considered as one period whereas the daytime period was considered separately for workdays (Saturday–Wednesday) and weekends (Friday).

The O_3 concentration prediction for the daytime period according to Equation (3) is best represented by:

$$[O_3]_{\text{daytime}} = \begin{cases} 1.09 \frac{[NO_2]}{[NO]} + 29.35 & \text{Workdays } (R^2 = 0.37) \\ 0.50 \frac{[NO_2]}{[NO]} + 35.47 & \text{Weekends } (R^2 = 0.31) \end{cases} \quad (8)$$

The predicted O_3 concentrations based on these equations are shown and compared to the measured ones in Figure 6. Note that the regression model parameters were obtained based on the 30-minutes average of the O_3 and NO_x data-base. In addition, the model predictions were also based

on the 30-minutes average of the concentrations and Figure 6 is based on averaging the results to obtain the daily patterns.

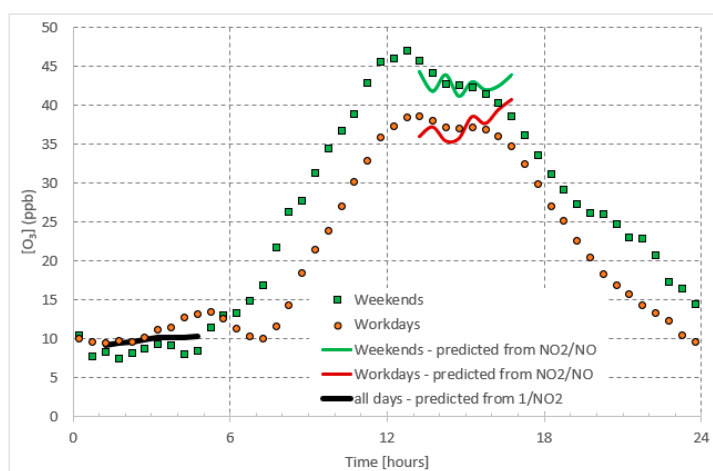


Figure 6. Prediction of daytime and night time O_3 concentrations compared with the measured ones.

Based on Equation (6), the α constant, which is supposed to be equivalent to J_{NO_2}/k_3 , is found to be 1.09 ppb and 0.50 ppb for workdays and weekends daytime, respectively. The δ constant, which is related to the background ozone concentrations, is 29.35 ppb and 35.47 ppb for workdays and weekends, respectively. The theoretical value of J_{NO_2}/k_3 calculated from the kinetics of the daytime reactions involved in O_3 formation at steady-state are presented by the function is found to be 8.7 ppb. This can be easily verified for J_{NO_2} provided by ACOM online database (http://cprm.acom.ucar.edu/Models/TUV/Interactive_TUV/) and substituting k_3 as proposed with Equation (2).

This means that α value is different than the ideal one represented by J_{NO_2}/k_3 . Note that the kinetic model represents the ideal case, when the concentration of O_3 depends solely on the NO_x - O_3 cycle with no contribution from additional sources or the involvement of other precursors in the O_3 formation processes. Additionally, the ideal case occurs in full solar exposure, without factors leading to solar radiation attenuation, including daytime PM and cloudiness. Also note that the additional parameter δ_1 can be thought of as a parameter that accounts for other processes contributing to the O_3 formation in Jeddah. Interestingly, the value of δ_1 is higher on weekends than on workdays. Other parameters which contribute to δ_1 include long range transport of O_3 , as well as stratosphere-troposphere O_3 migration. The latter is aided by the high temperature in Jeddah which enables this irreversible phenomenon to occur by increasing boundary layer height favoring proper mixing [41].

The O_3 concentration prediction for the nighttime period according to Equation (5) is best represented by,

$$[O_3]_{nighttime} = \frac{267.01}{[NO_2]} + 1.16 \quad \text{All days} (R^2 = 0.58) \quad (9)$$

The predicted O_3 concentrations are also shown and compared to the measured ones in Figure 6. Again, the regression model parameters were obtained based on the 30-minutes average of the O_3 and NO_x data-base.

This equation is based on the fact that NO_2 acts as a major sink for the night-time O_3 [24]. Here the parameter β can be thought of as the reaction rate of O_3 with NO_2 . In our analysis, β is rather similar for all days of the week and its value is about 267 ppb². The second parameter δ_2 has a value of 1.16 ppb. The theoretical value for the reaction rate of O_3 with NO_2 during nighttime is about 1250 ppb² [42–44]. Again, the deviations between β and the reaction rate of O_3 with NO_2 during nighttime can be explained by the occurrence of additional sinks of ozone, including surface reactions of particulate matter and deposition [24].

4. Conclusions

In this study, we suggested a simple statistical predictive model to calculate the steady-state daytime and nighttime O_3 concentrations at an urban coastal site. This model was formulated based on a modified approach of the null cycle of O_3 and NO_x . The model evaluation was performed by utilizing a one-year data-base of ozone (O_3) and nitrogen oxides (NO and NO_2) measured in Jeddah, which is located on the west coast of Saudi Arabia. The steady-state conditions for O_3 and NO_x at this site were observed during daytime (13:00–17:00) and nighttime (01:00–05:00).

The simple model for daytime concentrations was proposed to be linearly dependent on the concentration ratio of NO_2 to NO whereas that for the nighttime period it was suggested to be inversely proportional to NO_2 concentrations. Since the daytime O_3 concentrations on workdays (Saturday–Wednesday) were lower than those on weekends (Friday), two separate formulas were suggested for the daytime concentration predictions. Recalling the complex reactions involved in tropospheric O_3 formation, this proposed simple model provided reasonable predictions for the daytime and nighttime concentrations. Since the current description of the model is solely based on null cycle of O_3 and NO_x , other precursors should be considered in future development of this simple model.

Our study could be applied to several urban environments with similar emission patterns, as well as fill the gaps in O_3 data when no measurements were collected. Our study could also serve as basis for future studies for enforcing strategies to control ground level O_3 concentrations, as well as its precursors' emissions in polluted environments.

Author Contributions: Conceptualization, T.H., L.D., A.A.-H. and S.A.; Methodology, T.H. and L.D., A.A.-H.; Software, L.D., T.H., and M.A.Z.; Validation, L.D., T.H. and M.A.Z.; Formal Analysis, A.S.A., T.H., and L.D.; Investigation, M.K., H.A.-J., M.A.A., H.L., A.H., and T.H.; Resources, A.S.A., I.I.S., and F.M.A.; Data Curation, A.S.A., I.I.S., and F.M.A.; Writing-Original Draft Preparation, M.A.A., L.D. and T.H.; Writing-Review and Editing, M.A.A., L.D. and T.H.; Visualization, L.D., T.H. and M.A.Z.; Supervision, T.H.; Project Administration, M.K., H.A.-J., M.A.A., H.L., A.H., and T.H.; Funding Acquisition, H.A.-J. and M.A.A.

Funding: This research was funded by Deanship of Scientific Research (DSR) at King Abdulaziz University, Jeddah, under grant no. (I-122-30). The authors acknowledge with thanks DSR for technical and financial support. This study was also supported by the Academy of Finland Center of Excellence (grant no. 272041) and doctoral program in atmospheric sciences (ATM-DP).

Conflicts of Interest: The authors declare no conflict of interest.

References

1. WHO. *Health and Health Behaviour among Young People: Health Behaviour in School-Aged Children: A WHO Cross-National Study (HBSC), International Report*; WHO: Geneva, Switzerland, 2000.
2. IPCC. 2007: Summary for policymakers. In *Climate Change 2007: Impacts, Adaptation and Vulnerability. Contribution of Working Group II to the Fourth Assessment Report of the Intergovernmental Panel on Climate Change*; Cambridge University Press: Cambridge, UK, 2007; pp. 93–129.
3. Thompson, A.M. The oxidizing capacity of the Earth's atmosphere: Probable past and future changes. *Science* **1992**, *256*, 1157–1165. [[CrossRef](#)] [[PubMed](#)]
4. Laurila, T. Observational study of transport and photochemical formation of ozone over northern Europe. *J. Geophys. Res. Atmos.* **1999**, *104*, 26235–26243. [[CrossRef](#)]
5. Solomon, P.; Cowling, E.; Hidy, G.; Furiness, C. Comparison of scientific findings from major ozone field studies in North America and Europe. *Atmos. Environ.* **2000**, *34*, 1885–1920. [[CrossRef](#)]
6. Thompson, A.M.; Witte, J.C.; Hudson, R.D.; Guo, H.; Herman, J.R.; Fujiwara, M. Tropical tropospheric ozone and biomass burning. *Science* **2001**, *291*, 2128–2132. [[CrossRef](#)] [[PubMed](#)]
7. Pereira, M.; Alvim-Ferraz, M.; Santos, R. Relevant aspects of air quality in Oporto (Portugal): PM10 and O3. *Environ. Monit. Assess.* **2005**, *101*, 203–221. [[PubMed](#)]
8. Tecer, L.; Ertürk, F.; Cerit, O. Development of a regression model to forecast ozone concentration in Istanbul City, Turkey. *Fresenius Environ. Bull.* **2003**, *12*, 1133–1143.

9. Olszyna, K.; Luria, M.; Meagher, J. The correlation of temperature and rural ozone levels in southeastern USA. *Atmos. Environ.* **1997**, *31*, 3011–3022. [[CrossRef](#)]
10. Vingarzan, R.; Taylor, B. Trend analysis of ground level ozone in the greater Vancouver/Fraser Valley area of British Columbia. *Atmos. Environ.* **2003**, *37*, 2159–2171. [[CrossRef](#)]
11. Vukovich, F.M.; Sherwell, J. An examination of the relationship between certain meteorological parameters and surface ozone variations in the Baltimore–Washington corridor. *Atmos. Environ.* **2003**, *37*, 971–981. [[CrossRef](#)]
12. Ribas, À.; Peñuelas, J. Temporal patterns of surface ozone levels in different habitats of the North Western Mediterranean basin. *Atmos. Environ.* **2004**, *38*, 985–992. [[CrossRef](#)]
13. García, M.; Sánchez, M.; Pérez, I.; De Torre, B. Ground level ozone concentrations at a rural location in northern Spain. *Sci. Total Environ.* **2005**, *348*, 135–150. [[CrossRef](#)]
14. Dueñas, C.; Fernández, M.; Cañete, S.; Carretero, J.; Liger, E. Assessment of ozone variations and meteorological effects in an urban area in the Mediterranean Coast. *Sci. Total Environ.* **2002**, *299*, 97–113. [[CrossRef](#)]
15. Alvim-Ferraz, M.; Sousa, S.; Pereira, M.; Martins, F. Contribution of anthropogenic pollutants to the increase of tropospheric ozone levels in the Oporto Metropolitan Area, Portugal since the 19th century. *Environ. Pollut.* **2006**, *140*, 516–524. [[CrossRef](#)] [[PubMed](#)]
16. Pudasainee, D.; Sapkota, B.; Shrestha, M.L.; Kaga, A.; Kondo, A.; Inoue, Y. Ground level ozone concentrations and its association with NO_x and meteorological parameters in Kathmandu valley, Nepal. *Atmos. Environ.* **2006**, *40*, 8081–8087. [[CrossRef](#)]
17. Sillman, S. The use of NO_y, H₂O₂, and HNO₃ as indicators for ozone–NO_x–hydrocarbon sensitivity in urban locations. *J. Geophys. Res.* **1995**, *100*, 14175–14188. [[CrossRef](#)]
18. Nevers, N. Control of volatile organic compounds (VOCs). *Air Pollut. Control Eng.* **2000**, *18*, 329–330.
19. Sillman, S. The relation between ozone, NO_x and hydrocarbons in urban and polluted rural environments. *Atmos. Environ.* **1999**, *33*, 1821–1845. [[CrossRef](#)]
20. Guicherit, R.; Roemer, M. Tropospheric ozone trends. *Chemosphere-Glob. Chang. Sci.* **2000**, *2*, 167–183. [[CrossRef](#)]
21. Tang, W.; Zhao, C.; Geng, F.; Peng, L.; Zhou, G.; Gao, W.; Xu, J.; Tie, X. Study of ozone “weekend effect” in Shanghai. *Sci. China Ser. D Earth Sci.* **2008**, *51*, 1354–1360. [[CrossRef](#)]
22. Song, F.; Shin, J.Y.; Jusino-Atresino, R.; Gao, Y. Relationships among the springtime ground-level NO_x, O₃ and NO₃ in the vicinity of highways in the US East Coast. *Atmos. Pollut. Res.* **2011**, *2*, 374–383. [[CrossRef](#)]
23. Domínguez-López, D.; Adame, J.; Hernández-Ceballos, M.; Vaca, F.; De la Morena, B.; Bolívar, J. Spatial and temporal variation of surface ozone, NO and NO₂ at urban, suburban, rural and industrial sites in the southwest of the Iberian Peninsula. *Environ. Monit. Assess.* **2014**, *186*, 5337–5351. [[CrossRef](#)] [[PubMed](#)]
24. Finlayson-Pitts, B.J.; Pitts, J.N., Jr. *Chemistry of the Upper and Lower Atmosphere: Theory, Experiments, and Applications*; Academic Press: Cambridge, MA, USA, 1999.
25. Rao, T.; Reddy, R.; Sreenivasulu, R.; Peeran, S.; Murthy, K.; Ahammed, Y.; Gopal, K.; Azeem, P.; Sreedhar, B.; Sunitha, K. Air space pollutants CO and NO_x level at Anantapur (semi-arid zone), Andhra Pradesh. *J. Indian Geophys. Union* **2002**, *3*, 151–161.
26. Rao, T.; Reddy, R.; Sreenivasulu, R.; Peeran, S.; Murthy, K.; Ahammed, Y.; Gopal, K.; Azeem, P.; Sreedhar, B.; Badarinath, K. Seasonal and diurnal variations in the levels of NO_x and CO trace gases at Anantapur in Andhra Pradesh. *J. Indian Geophys. Union* **2002**, *3*, 163–168.
27. Vingarzan, R. A review of surface ozone background levels and trends. *Atmos. Environ.* **2004**, *38*, 3431–3442. [[CrossRef](#)]
28. Chameides, W.; Fehsenfeld, F.; Rodgers, M.; Cardelino, C.; Martinez, J.; Parrish, D.; Lonneman, W.; Lawson, D.; Rasmussen, R.; Zimmerman, P. Ozone precursor relationships in the ambient atmosphere. *J. Geophys. Res. Atmos.* **1992**, *97*, 6037–6055. [[CrossRef](#)]
29. Lal, S.; Naja, M.; Subbaraya, B. Seasonal variations in surface ozone and its precursors over an urban site in India. *Atmos. Environ.* **2000**, *34*, 2713–2724. [[CrossRef](#)]
30. Mazzeo, N.A.; Venegas, L.E.; Choren, H. Analysis of NO, NO₂, O₃ and NO_x concentrations measured at a green area of Buenos Aires City during wintertime. *Atmos. Environ.* **2005**, *39*, 3055–3068. [[CrossRef](#)]
31. Han, S.; Bian, H.; Feng, Y.; Liu, A.; Li, X.; Zeng, F.; Zhang, X. Analysis of the Relationship between O₃, NO and NO₂ in Tianjin, China. *Aerosol Air Qual. Res.* **2011**, *11*, 128–139. [[CrossRef](#)]

32. Abdul-Wahab, S.A.; Bakheit, C.S.; Al-Alawi, S.M. Principal component and multiple regression analysis in modelling of ground-level ozone and factors affecting its concentrations. *Environ. Model. Softw.* **2005**, *20*, 1263–1271. [[CrossRef](#)]
33. Sousa, S.; Martins, F.; Alvim-Ferraz, M.; Pereira, M.C. Multiple linear regression and artificial neural networks based on principal components to predict ozone concentrations. *Environ. Model. Softw.* **2007**, *22*, 97–103. [[CrossRef](#)]
34. Özbay, B.; Keskin, G.A.; Doğruparmak, Ş.Ç.; Ayberk, S. Multivariate methods for ground-level ozone modeling. *Atmos. Res.* **2011**, *102*, 57–65. [[CrossRef](#)]
35. Varotsos, C.; Ondov, J.; Efstathiou, M. Scaling properties of air pollution in Athens, Greece and Baltimore, Maryland. *Atmos Environ.* **2005**, *39*, 4041–4047.
36. Alghamdi, M.; Khoder, M.; Harrison, R.M.; Hyvärinen, A.-P.; Hussein, T.; Al-Jeelani, H.; Abdelmaksoud, A.; Goknil, M.; Shabbaj, I.; Almeahadi, F. Temporal variations of O₃ and NO_x in the urban background atmosphere of the coastal city Jeddah, Saudi Arabia. *Atmos. Environ.* **2014**, *94*, 205–214. [[CrossRef](#)]
37. Leighton, P. *Photochemistry of Air Pollution*; Elsevier: New York, NY, USA, 2012.
38. Seinfeld, J.H.; Pandis, S.N. *Atmospheric Chemistry and Physics: From Air Pollution to Climate Change*; John Wiley & Sons: Hoboken, NJ, USA, 2016.
39. Khodeir, M.; Shamy, M.; Alghamdi, M.; Zhong, M.; Sun, H.; Costa, M.; Chen, L.-C.; Maciejczyk, P. Source apportionment and elemental composition of PM_{2.5} and PM₁₀ in Jeddah City, Saudi Arabia. *Atmos. Pollut. Res.* **2012**, *3*, 331. [[CrossRef](#)] [[PubMed](#)]
40. Marr, L.C.; Harley, R.A. Modeling the effect of weekday-weekend differences in motor vehicle emissions on photochemical air pollution in central California. *Environ. Sci. Technol.* **2002**, *36*, 4099–4106. [[CrossRef](#)]
41. Kuang, S.; Newchurch, M.; Burris, J.; Wang, L.; Knupp, K.; Huang, G. Stratosphere-to-troposphere transport revealed by ground-based lidar and ozonesonde at a midlatitude site. *J. Geophys. Res. Atmos.* **2012**, *117*. [[CrossRef](#)]
42. Cox, R.; Coker, G. Kinetics of the reaction of nitrogen dioxide with ozone. *J. Atmos. Chem.* **1983**, *1*, 53–63. [[CrossRef](#)]
43. Huie, R.E.; Herron, J.T. The rate constant for the reaction O₃ + NO₂ → O₂ + NO₃ over the temperature range 259–362 K. *Chem. Phys. Lett.* **1974**, *27*, 411–414. [[CrossRef](#)]
44. Johnston, H.S.; Graham, R. Photochemistry of NO_x and HNO_x compounds. *Can. J. Chem.* **1974**, *52*, 1415–1423. [[CrossRef](#)]

